AGU ADVANCING EARTH AND SPACE SCIENCE

Geophysical Research Letters®

RESEARCH LETTER
10.1029/2021GL096120

The Influence of the Trend, Basin Interactions, and Ocean Dynamics on Tropical Ocean Prediction

Michael A. Alexander[1], Sang-Ik Shin[1,2], and David S. Battisti[3]

[1]NOAA Physical Sciences Laboratory, Boulder, CO, USA, [2]CIRES, University of Colorado Boulder, Boulder, CO, USA, [3]Department of Atmospheric Sciences, University of Washington, Seattle, WA, USA

Key Points:

- A set of empirical models are used to examine processes that affect forecasts of sea surface temperature and height in the tropical oceans
- The trend and El Niño-Southern Oscillation (ENSO) strongly affect forecast skill in the Indian and north tropical Atlantic oceans
- The tropical Atlantic and Indian Oceans influence ENSO and other parts of the Pacific at forecast leads >6 months

Supporting Information:

Supporting Information may be found in the online version of this article.

Correspondence to:

M. A. Alexander,
michael.alexander@noaa.gov

Citation:

Alexander, M. A., Shin, S.-I., & Battisti, D. S. (2022). The influence of the trend, basin interactions, and ocean dynamics on tropical ocean prediction. *Geophysical Research Letters*, *49*, e2021GL096120. https://doi.org/10.1029/2021GL096120

Received 15 SEP 2021
Accepted 12 JAN 2022

Author Contributions:

Conceptualization: Michael A. Alexander, Sang-Ik Shin, David S. Battisti
Formal analysis: Michael A. Alexander, Sang-Ik Shin
Investigation: Michael A. Alexander, Sang-Ik Shin
Methodology: Sang-Ik Shin, David S. Battisti
Project Administration: Michael A. Alexander
Software: Sang-Ik Shin
Validation: Sang-Ik Shin, David S. Battisti
Visualization: Michael A. Alexander, Sang-Ik Shin
Writing – original draft: Michael A. Alexander, Sang-Ik Shin

Abstract The trend, connections between tropical ocean basins and dynamical processes on sea surface temperature (SST) and sea surface height (SSH) forecast skill are investigated using a linear inverse model (LIM) framework. The warming trend has a strong influence on 6-month SST forecast skill in the Indian Ocean, Western Pacific, and north tropical Atlantic, but little effect on El Niño-Southern Oscillation (ENSO) prediction. ENSO strongly impacts the SST forecast skill in all three ocean basins including most of the Indian Ocean and the north tropical Atlantic. Without interactions with the Indian Ocean, the 6-month SST forecast skill is substantially reduced in the western tropical Pacific and SSH skill decreases in the central Pacific. Atlantic and Indian Ocean interactions with the Pacific enhance ENSO forecast skill at 6–12 months leads. The Indian Ocean influences SSH in the eastern Atlantic, while the tropical Atlantic affects SST forecasts in portions of the Indian Ocean.

Plain Language Summary Predicting ocean conditions is important for marine ecosystem management and because the ocean temperatures, especially in the tropics, strongly influence weather patterns on seasonal time scales. Here, we use a statistical model to examine how processes, such as the long term trend and interactions between the tropical Atlantic, Pacific, and Indian oceans influence forecast skill. Warming of the ocean strongly influences 6-month sea surface temperature forecasts over most of the Indian Ocean and the North tropical Atlantic but not in the central and eastern Pacific. Variability in the tropical Pacific Ocean, much of which is associated with the El Niño-Southern Oscillation (ENSO) phenomena, strongly influences forecast skill in all three ocean basins. Both the tropical Atlantic and Indian oceans were found to influence 6–12 month ENSO forecasts. Our study also revealed additional connections between oceans including the Indian Ocean's influence on the eastern Atlantic and the Atlantic's influence on portions of the Indian Ocean and in the Pacific off the South American coast, although some of the connections may be associated with the longer term trend.

1. Introduction

The tropical oceans are influenced by multiple processes including long-term trends associated with global warming, ocean dynamics including oceanic Rossby and Kelvin waves, and air-sea interactions both within and between ocean basins. These processes drive seasonal to interannual variability as well as decadal trends in the tropical oceans as indicated by changes in sea surface temperature (SST) and sea surface height (SSH). Examples of the ocean variability include the long-term warming of the tropical Indian Ocean, primarily in response to increasing greenhouse gasses (Dong et al., 2014; Du & Xie, 2008); SST oscillations on 2–7 yr time scales in the tropical Pacific associated with El Niño-Southern Oscillation (ENSO; e.g., Neelin et al., 1998; Wang et al., 2017) and the "atmospheric bridge," where ENSO-driven atmospheric teleconnections influence remote air-sea interactions, including the tropical Indian and Atlantic oceans (e.g., Alexander et al., 2002; Chiang & Sobel, 2002; Klein et al., 1999).

Interactions between tropical ocean basins have been well studied, as recently reviewed by Wang (2019), Cai et al. (2019), and Keenlyside et al. (2020). The atmospheric bridge acts to warm the northern Tropical Atlantic Ocean in boreal spring following an ENSO event (Curtis & Hastenrath, 1995; Enfield & Mayer, 1997), while it is a main driver of the Indian Ocean dipole during boreal summer and fall when ENSO events begin, and basin-wide anomalies when events peak in winter (Baquero-Bernal et al., 2002; Shinoda, Alexander, & Hendon, 2004). ENSO-driven variability in the Indian Ocean is due to changes in surface fluxes and to ocean dynamics, including changes in upwelling west of Indonesia and wind-driven Rossby waves (Chambers et al., 1999; Shinoda, Hendon, & Alexander, 2004; Xie et al., 2002). While ENSO is primarily governed by air-sea interaction in the

Writing – review & editing: Michael A. Alexander, David S. Battisti

tropical Pacific, Indian, and Atlantic SSTs influence the Pacific including the timing, position, and amplitude of ENSO events (e.g., Annamalai et al., 2005; Ding et al., 2011; Dommenget & Yu, 2017; Ham et al., 2013; Rodriguez-Fonesca et al., 2009; Ruprich-Robert et al., 2017; Wu & Kirtman, 2004). Coupled interactions between the tropical Indian and Atlantic Ocean basins may also occur (Kajtar et al., 2017).

The role of tropical basin interactions on potential predictability and actual predictions of ocean conditions has received less attention in the literature. Using coupled ocean-atmospheric general circulation models (AGCMs), Frauen and Dommenget (2012) and Keenlyside et al. (2013), found that the tropical Atlantic influenced ENSO predictability. Results from studies of the Indian Ocean's influence on ENSO forecasts are mixed, with some showing strong effects (Izumo et al., 2010; Luo et al., 2010; Zhou et al., 2019), while others found little impact (Frauen & Dommenget, 2012; Jansen et al., 2009). Forecasts from an AGCM-ocean mixed layer model indicated that global SST anomalies enhanced SST forecast skill in the north tropical Atlantic, relative to forecasts initialized with just Atlantic SSTs (Chang et al., 2003). Penland and Matrosova (1998) found that including SST anomalies in the tropical Indo-Pacific enhanced SST forecast skill in the north tropical Atlantic and Caribbean Sea, based on results from observation-based linear inverse models (LIMs). Here, we also use the LIM framework, expanding on the work by Penland and Matrosova, by (a) including interactions between all three tropical basins, (b) including SSH in addition to SST, and (c) exploring the role of the trend, connections among ocean basins, and dynamical processes in the Indian and Atlantic oceans on forecast skill.

2. Methods and Data

2.1. Linear Inverse Model

Linear Inverse models have been used in a wide array of climate applications, including predictions of tropical ocean conditions (e.g., Newman & Sardeshmukh, 2017; Penland & Sardeshmukh, 1995). A LIM can be expressed as:

$$\frac{d\mathbf{x}}{dt} = \mathbf{L}\mathbf{x} + \mathbf{S}\boldsymbol{\eta}, \tag{1}$$

where $\mathbf{x}$ is the state vector, $\mathbf{L}$ is the linear matrix operator that provides the deterministic evolution of the system, and $\mathbf{S}\boldsymbol{\eta}$ is the stochastic noise, which is white in time but can have spatial structure. The matrix $\mathbf{L}$ can be estimated from the concurrent and lagged covariances, $\mathbf{C}(0)$ and $\mathbf{C}(\tau_0)$, $\mathbf{L} = \tau_0^{-1}\ \ln[\mathbf{C}(\tau_0)\mathbf{C}(0)^{-1}]$, where the lag τ_0 is set to 1 month in this study. Given the necessity of having long data records to accurately represent seasonally varying $\mathbf{L}$ and $\mathbf{S}$ values (Shin et al., 2021), we assumed that they are state-independent; and thus, the ensemble mean forecasts at lead τ can be obtained from

$$\mathbf{x}(t+\tau) = \mathbf{G}(\tau)\mathbf{x}(t), \tag{2}$$

where $\mathbf{G}(\tau) = \exp(\mathbf{L}\tau)$ is the linear system propagator.

We obtained monthly SST and SSH values on a $1° \times 1°$ grid for the years 1965–2014 from the HadISST v1 data set (Rayner et al., 2003) and ORAS4 ocean reanalysis (Balmaseda et al., 2015), respectively. In our LIM, monthly SST and SSH anomalies in each basin are treated as separate variables and the state vector $\mathbf{x}$ and operator $\mathbf{L}$ can be expressed as:

$$\mathrm{x} = \begin{pmatrix} \mathrm{SST_{TI}} \\ \mathrm{SST_{TI}} \\ \mathrm{SST_{TP}} \\ \mathrm{SST_{TP}} \\ \mathrm{SST_{TA}} \\ \mathrm{SST_{TA}} \end{pmatrix} \quad \text{and} \quad \mathbf{L} = \begin{bmatrix} \mathrm{L_{TI\text{-}TI}} & \mathrm{L_{TI\text{-}TP}} & \mathrm{L_{TI\text{-}TA}} \\ \mathrm{L_{TP\text{-}TI}} & \mathrm{L_{TP\text{-}TP}} & \mathrm{L_{TP\text{-}TA}} \\ \mathrm{L_{TA\text{-}TI}} & \mathrm{L_{TA\text{-}TP}} & \mathrm{L_{TA\text{-}TA}} \end{bmatrix}, \tag{3}$$

where subscripts TI, TP, and TA indicate the tropical Indian, Pacific, and Atlantic oceans (Figure 1). Submatrices $\mathbf{L}_{A\text{-}B}$ represent the interactions between two basins, that is, the impact of basin B on basin A. Interaction between basins A and B are further decomposed as:

$$\mathbf{L}_{A\text{-}B} = \begin{bmatrix} \mathbf{L}_{SST(A)\text{-}SST(B)} & \mathbf{L}_{SST(A)\text{-}SSH(B)} \\ \mathbf{L}_{SSH(A)\text{-}SST(B)} & \mathbf{L}_{SSH(A)\text{-}SSH(B)} \end{bmatrix}, \quad (4)$$

where element $\mathbf{L}_{x(A)\text{-}y(B)}$ denotes the impact of the variable y in basin B on variable x in basin A. Following Newman (2007), Zhang et al. (2021), and Zhao et al. (2021), the effects of coupling between basins can be removed by setting the interaction submatrices = 0. Intra-basin terms can also be suppressed by setting the relevant elements to zero.

Following Penland and Matrosova (1998), the LIM framework is also used to design filters for the trend and ENSO-related variability. The filters (see Text S1 in Supporting Information S1) involve finding the empirical normal modes (ENMs), the solutions to the deterministic portion of the LIM. The trend filter is obtained from a single least-damped ENM. The ENSO filter is derived from the pairs of modes (ENMs 4/5 and 9/10) that project onto the initial "optimal structure," the anomaly pattern that exhibits maximum growth of the anomaly variance over time, and gives rise to an ENSO event ~6 months later.

To identify significant large-scale patterns, EOFs normalized by their basin-wide standard deviation, were computed in each domain. The leading three, five, and seven SST and SSH EOFs were retained in the Atlantic, Indian, and Pacific oceans, which explain 66.5/66.2, 71.9/64.1, and 79.5/71.8, of the total SST/SSH variance, respectively. The number of EOFs were chosen to maximize skill over the entire tropics, which resulted in using the same number of SST and SSH EOFs in each basin. The principal components, the time-varying EOF coefficients, comprise the 30-component state vector **x** in Equation (3).

2.2. Model Experiments Using Reduced LIMs

The LIM framework allows us to isolate the influence of ocean variability and dynamics on SST and SSH predictions. By comparing reduced LIMs with the full LIM we can investigate the role of:

1. The trend—By removing SST and SSH anomalies associated with the first ENM; using a large ensemble of GCM simulations, Frankignoul et al. (2017) found that using ENM1 from a LIM was an effective way to identify and remove the long-term anthropogenic forcing, although our focus is on the influence of the trend on forecast skill rather than its cause.
2. ENSO—By removing SST and SSH anomalies associated with ENMs 4/5 and 9/10, which greatly reduces the SST anomalies in the NINO3.4 region (5°N–5°S, 170°E–120°W) as shown by the full and filtered NINO3.4 time series and power spectra (Figure S4 in Supporting Information S1).
3. Basin interactions—Disabling communication between basins by setting the SST and SSH basin interaction coefficients ($\mathbf{L}_{A\text{-}B}$) in Equation (3) to zero
4. Reduced ocean dynamics in the Atlantic and Indian oceans—"No-SSH" forecasts by setting the the SSH $\mathbf{L}$ elements within and between basins to zero in Equation (4).

The SST and SSH forecasts are cross-validated by sub-sampling the data by successively removing 5-yr segments (10% of data) at a time, re-estimating $\mathbf{L}$ (and thereby $\mathbf{G}$) using the remaining 45 independent years. Then 12-month forecasts are generated via Equation (2) for each calendar month during the independent years. Forecasts are bench-marked against the untruncated (in EOF space) observations during 1965–2014 and forecast skill is evaluated using local anomaly correlation (AC) and root-mean-square error (RMSE) based skill score ($RMSSS = 1 - RSME_{forecast}/RSME_{Climate}$; Barnston et al., 2015). We computed the statistical significance (95% confidence level) of the difference between the AC values in the full and reduced LIMs using a moving block bootstrap Monte Carlo method (Efron & Tibshirani, 1993) with 2,000 samples. RMSSS skill maps (Figures S5–S7) are largely consistent with those for AC shown in Section 3.

3. Results

The full LIM has considerable skill in predicting SST and SSH anomalies at a 6-month lead in portions of the three basins, consistent with previous LIM forecasts (e.g., Newman & Sardeshmukh, 2017; Shin et al., 2021). AC values exceed 0.6 for SST in the central tropical Pacific and Indian oceans and the western Atlantic. There is high forecast skill for SSH in the vicinity of the Maritime Continent from the west Pacific to the eastern Indian Ocean, the eastern TP in the Southern Hemisphere, and most of the TA (Figure 1a). Removing the trend substantially reduces the LIM's SST prediction skill in the Indian and Atlantic oceans with little change in the ENSO region, consistent with Ding et al. (2019). The skill of the detrended 6-month SSH forecasts decreases substantially throughout the TA and to a lesser degree in the western TP and southeastern TI (Figure 1b). After removing both the trend and ENSO variability the forecast skill is much lower over all three basins, with AC > 0.4 only in small areas of the eastern Pacific in the Southern Hemisphere for SST and the subtropics in both hemispheres for SSH (Figure 1c).

The change in the 6-month forecast skill resulting from the removal of basin interactions is explored in Figure 2 (see Figure S8 in Supporting Information S1 when the data are detrended prior to decoupling). Eliminating interactions between all three basins results in a substantial loss of SST forecast skill in the Indian Ocean, with AC values decreasing by 0.4 in all but the eastern TI (Figure 2a). Significant decreases in SST AC occur in the western and eastern Pacific and portions of the tropical Atlantic, with little change in the central Pacific. Removing all basin interactions also reduces SSH forecast skill, especially in the Arabian Sea and east of Madagascar in the Indian Ocean and in the eastern Pacific around 15°S. Most of the reduction in SST and SSH skill results from the interactions between the TP and the other two basins (Figure 2b). Removing TI interactions greatly reduced SST skill in that basin and the far western Pacific, and reduced SSH skill in the central equatorial Pacific and along the equator and the far eastern Atlantic (Figure 2c). There are also reductions in AC values (−0.2 to −0.4) in portions of the equatorial and southeast Pacific and Atlantic. Removing the TI interactions has a much stronger effect on 12 months TP forecasts (not shown but see Figure 4). Removing TA interactions reduced SST skill within the basin and in the equatorial and eastern Indian Ocean, with more modest reductions in the southeast Pacific; SSH skill is reduced in the southeastern TP (Figure 2d). There are some regions where skill increases when removing interactions, but they are generally not significant.

Removing the SSH variability in the TI and TA has a modest impact on SST forecast skill throughout the tropics, including the entire TA (Figure 3a). Surprisingly, the largest decrease in both SST and SSH forecast skill occurs to the west of Central and South America, especially in the vicinity of 15°S. The AC slightly decreases in the vicinity of the Maritime Continent and at ∼20°S in the central Indian Ocean. Removing the trend in addition to removing TI and TA SSH variability (Figure 3b) further decreases the SSH skill relative to the detrended LIM on both sides of the equator in the central Pacific. The decrease in SSH skill off South America in the no-SSH

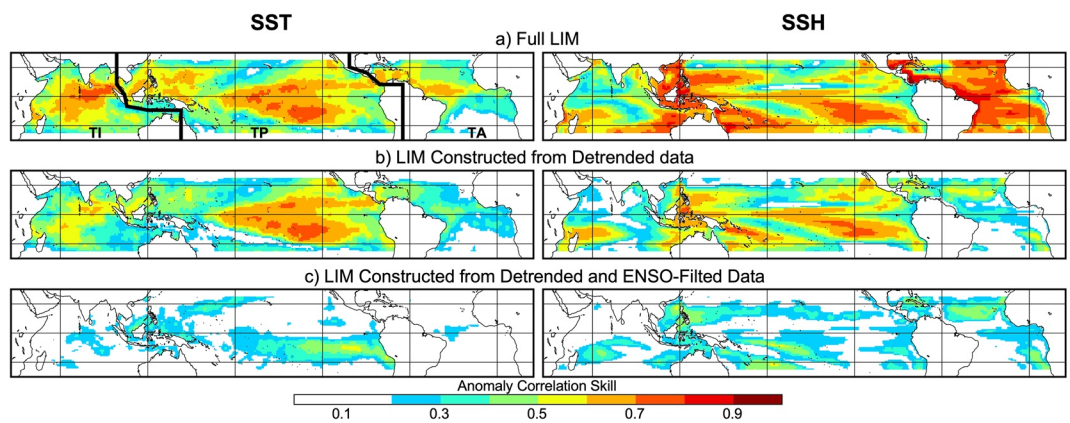

Figure 1. Hindcast skill as indicated by the anomaly correlation between the 6-month lead LIM forecasts and observations for SST (left) and SSH (right) over the period 1964–2004. (a) Full LIM, (b) LIM constructed from detrended data (removal of ENM 1), and (c) LIM constructed from detrended and ENSO-filtered data (removal of ENMs 1, 4/5, and 9/10). (Top left) The tropical Indian (TI), Pacific (TP), and Atlantic (TA) ocean domains are separated by thick black lines. Latitude lines are shown at 20°N, 0°, and 20°S.

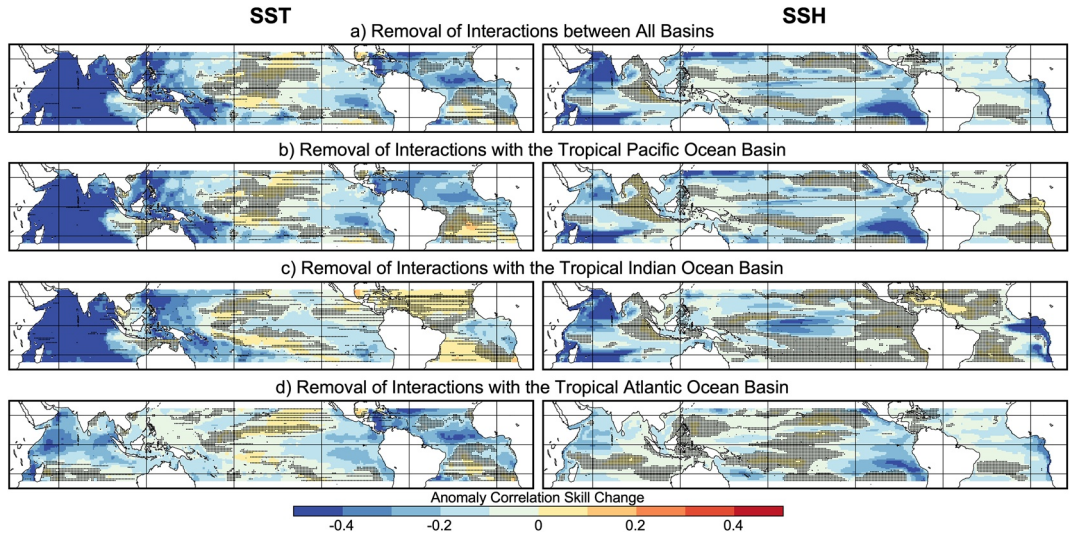

Figure 2. The change in the 6-month (left) SST and (right) SSH forecast skill due to basin interactions as indicated by the difference in the anomaly correlation between the full LIM and LIMs by the removal of all interactions: (a) between all basins; (b) with the tropical Pacific (TP); (c) with tropical Indian (TI); and (d) with tropical Atlantic (TA) ocean basins. Grid squares that are *not* significant at the 95% level are hatched.

experiment is much weaker when the trend is also removed, although there is little impact on the SST skill in that region.

Next, we examine the influence of the trend, basin interactions, and SSH variability on LIM SST forecasts for the NINO 3.4 region (5°N–5°S, 170°E–120°W). The skill, as indicated by the AC and RMSSS, is shown as a function of verification month and lead time in Figure 4. Both skill measures indicate the full LIM performs well for forecasts that verify in October-March, with AC (RMSSS) values greater than 0.8 (0.5) and 0.6 (0.2) at lead times of up to 4 and 9 months, respectively. The skill is much lower for forecasts that verify in April–September—crossing boreal spring, associated with the "spring persistence barrier," when forecasts from both dynamical and empirical models exhibit limited ENSO prediction skill (e.g., Levine & McPhaden, 2015; Liu et al., 2019; Torrence & Webster, 1998; Wright, 1979). Removing the trend has almost no impact on forecast skill (Figure 4b), while by design, removing the ENSO modes greatly reduces the skill (Figure 4c).

Removing the interactions between the Pacific and the other two basins reduces the NINO3.4 SST skill for forecasts verifying in May–October starting at leads of ~6 months (Figure 4d). Thus, without basin interactions, ENSO forecast skill would be even lower in boreal summer and early fall. The reduction in both skill metrics exhibit a slope that occurs later in the year at longer leads, with the largest decrease in AC occurring from August to November at leads of 8–12 months and the maximum decrease in RMSSS during June–August at 7–9 months leads. TI-TP interactions influence ENSO forecast skill at leads of more than ~4 months, which increases with

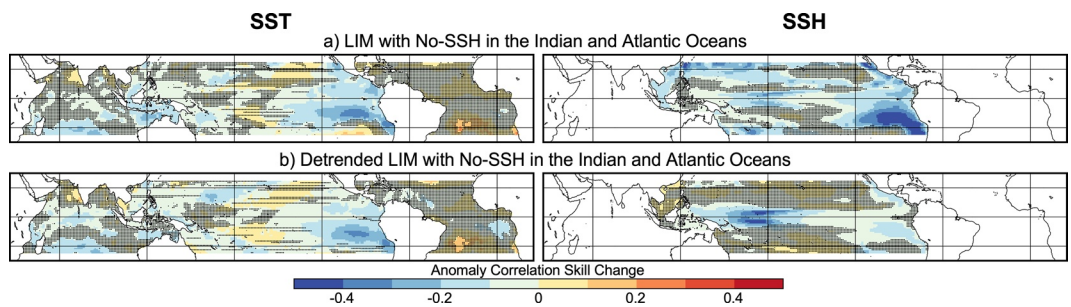

Figure 3. The change in the 6-month (left) SST and (right) SSH hindcast skill as indicated by the difference in the anomaly correlation between the full LIM and a LIM (a) with removal of all SSH terms in the Indian and Atlantic Oceans; (b) using the detrended LIM with no SSH anomalies in the Indian and Atlantic oceans. Non-significant values are hatched.

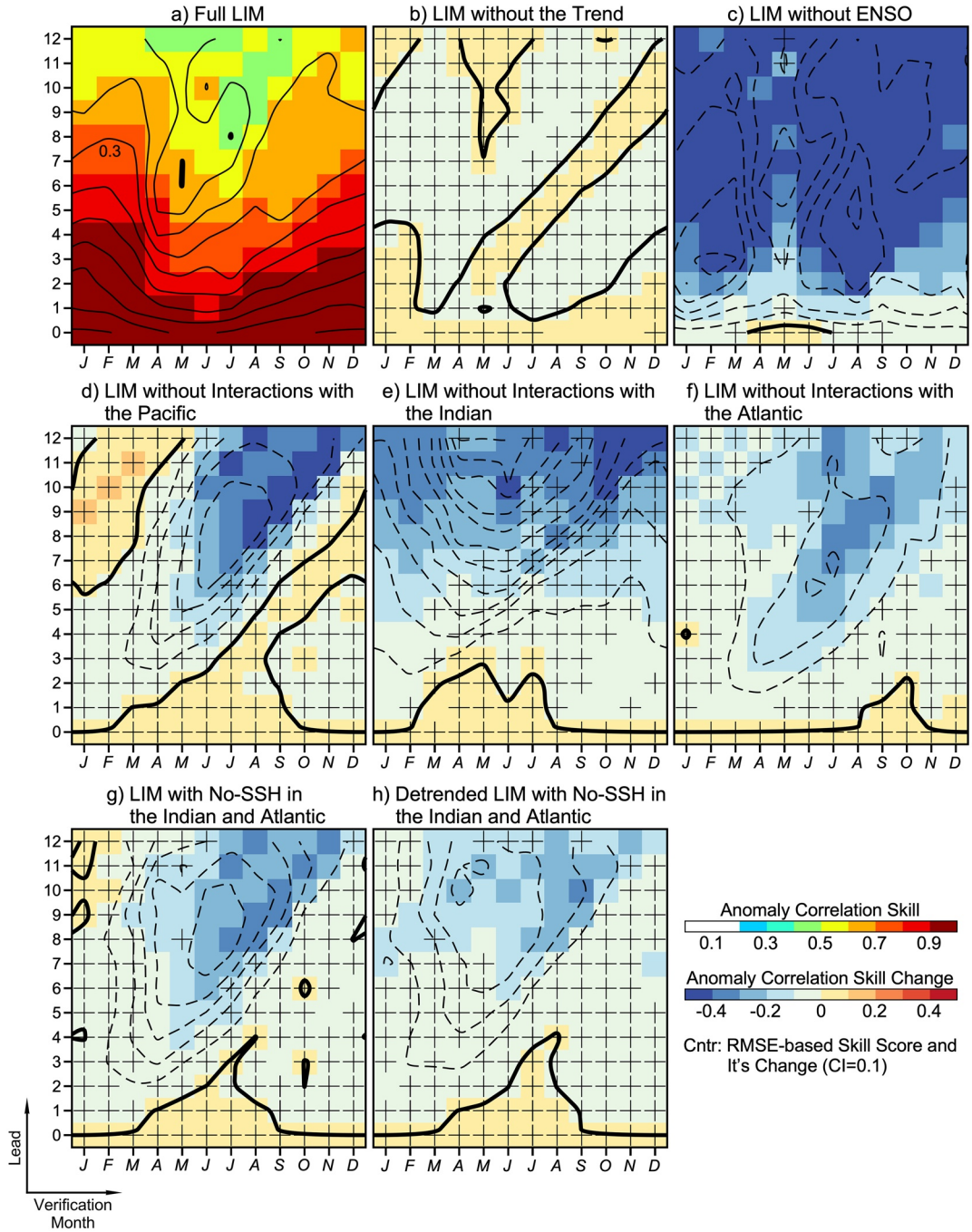

Figure 4. Hindcast skill of SST anomaly in the NINO 3.4 region (5°N–5°S, 170°E–120°W) as indicated by the AC (shaded) and RMSSS (contours, interval = 0.1, zero contour—thick solid line) as a function of verification month (*x*-axis) and lags of up to 12 months (*y*-axis). (a) Skill of the full LIM; (b)–(h) difference in skill (AC bottom shade scale, RMSSS interval 0.1, zero line thick solid line, negative values dashed) between the full LIM and altered LIMs: (b) without the trend; (c) without ENSO; (d) without interactions between the Pacific and other basins; (e) without interactions with the Indian Ocean; (f) without interactions with the Atlantic; (g) no SSH variability in the Indian and Atlantic oceans; (h) as in (g) but with the trend removed. Non-significant values are indicated by +signs.

lead, although whether a change in AC is significant varies by lead and verification month (Figure 4e). The largest decrease occurs in summer for RMSSS but without a strong seasonal signal for AC, when TI is decoupled. When the TA and TP are decoupled ENSO forecast skill decreases especially for forecasts that verify in boreal summer at leads of ≥5 months (Figure 4f), indicating that interactions with the Atlantic reduces the spring predictability

barrier, consistent with Keenlyside et al. (2013). The change in skill resulting from removing SSH anomalies in the TI and TA (Figure 4g) resembles the LIM without interactions with the tropical Pacific (Figure 4d) but with reduced amplitude, indicating that SSH-related variability in the Atlantic and Indian oceans has some influence the forecasts of ENSO SST anomalies, especially at longer leads from March to November. The change in skill in the detrended/no-SSH LIM (Figure 4h, which is relative to the detrended LIM) exhibits a similar pattern as the no-SSH LIM but overall the decrease in skill is reduced after detrending.

4. Summary and Discussion

We examined the role of the trend, ENSO, connections between ocean basins and dynamical processes in the Indian and Atlantic oceans on tropical SST and SSH forecast skill based on a linear inverse model and a set of reduced LIMs. The warming trend has a strong influence on the 6-month SST forecast skill in the Indian Ocean, western Pacific, and north tropical Atlantic but negligible effects on the central and eastern Pacific and thus ENSO prediction. The trend also strongly affects 6-month SSH forecasts throughout the tropical Atlantic and over the Maritime Continent/western Pacific. While some skill may come from predicting the trend during the forecast period, it primarily arises due to the conditions at initiation relative to the long-term climatology (Ding et al., 2019).

ENSO strongly impacts the 6-month SST forecast skill in all three basins: without ENSO and the trend there is almost no forecast skill in the Atlantic and Indian oceans and only limited skill in the Pacific south of the equator and east of the dateline. The remote influence of ENSO and tropical Pacific variability in general is further confirmed when basin interactions are removed, which results in a strong drop in skill throughout the Indian Ocean and the north tropical Atlantic. The influence of the TP on these regions primarily occurs through the "atmospheric bridge," where ENSO-driven atmospheric teleconnections influence the surface fluxes in remote ocean basins (e.g., Alexander et al., 2002).

Without interactions with the Indian Ocean, the SST forecast skill is substantially reduced in the western tropical Pacific and in the ENSO region at leads of more than ~5 months. Zhang et al. (2021) also used a LIM-based ocean decoupling approach and found that the Indian Ocean SSTs, especially those associated with the dipole mode, influenced tropical Pacific SST variability and would thus impact ENSO forecast skill. The influence of the Indian Ocean dipole on ENSO may occur in the ocean via the Indonesian throughflow (Yuan et al., 2011, 2013), in addition to the atmosphere. In our LIM analysis, the TI also influences the SSH skill between approximately 5°N–5°S in the central Pacific. SSH anomalies in this region could be indicative of Kelvin and near-equatorial Rossby waves. The subsequent propagation of these waves could influence ENSO over the subsequent months to multiple seasons, respectively (e.g., Battisti et al., 2018). This may partly explain why removing TI interactions substantially reduces ENSO forecast skill at longer lead times (Figure 4e). Since ENSO is partly cyclic, relationships at longer leads with anomalies in other basins may reflect conditions that are actually driven by ENSO, rather than indicating an independent ENSO precursor. The remote SST anomalies, however, may also feedback on ENSO (Zhang et al., 2021).

The LIM framework suggests other intriguing interactions between basins, including the influence of the TI on SSH in the eastern Atlantic and of the TA on SSTs along the equator and in the western part of the Indian Ocean. Including Atlantic and Indian Ocean interactions enhance SST forecast skill in the eastern Pacific and substantially increase the SSH prediction skill west of South America around 15°S. The underlying dynamics for the latter source of skill is unclear but it may be related to the trend rather than direct interbasin connections (see Figure S8 in Supporting Information S1) or result from $\mathbf{L}$ not varying with the seasons (Shin et al., 2021). Removing SSH variability in the Indian and Atlantic Oceans has limited impact on the 6-month SST forecast skill throughout the tropics and on 6–12 months ENSO forecasts, suggesting an important role for thermodynamic processes within the Indian and Atlantic oceans and in basin interactions.

While LIM is a linear system (nonlinearities are treated as stochastic noise), modal interference cause the anomaly patterns to vary in space and time. As a result, the forecast skill may not simply result from the linear addition of two or more processes. For example, NINO3.4 SST forecast skill slightly increases for forecasts that verify in January–March at leads ≥7 months when interactions between the Pacific and the two other ocean basins are removed in tandem (Figure 4d); in contrast, removing the TP-TI and TP-TA interactions separately (Figures 4e and 4f) and then summing their effects would act to decrease the forecast skill for these months/leads. Thus,

interaction between processes, including connections between basins, can have a complex influence on forecasts. Including state dependence, such as multiplicative noise and/or seasonal variations in and in a LIM, or using deterministic nonlinear predictors, may improve the representation of processes and thus seasonal forecasts (e.g., Chen et al., 2016; Martinez-Villalobos et al., 2019; Shin et al., 2021).

Data Availability Statement

HadISST data are available at https://www.metoffice.gov.uk/hadobs/hadisst/data/download.html; ECMWF ORAS4 data are available at: http://apdrc.soest.hawaii.edu/datadoc/ecmwf_oras4.php.

Acknowledgments
We thank Matt Newman and the two anonymous reviewers for their comments and suggestions. This work was supported by the NOAA precipitation grand challenge initiative.

References

Alexander, M. A., Bladé, I., Newman, M., Lanzante, J. R., Lau, N. C., & Scott, J. D. (2002). The atmospheric bridge: The influence of ENSO teleconnections on air-sea interaction over the global oceans. *Journal of Climate*, *15*(16), 2205–2231. https://doi.org/10.1175/1520-0442(2002)015<2205:TABTIO>2.0.CO;2

Annamalai, H., Xie, S. P., McCreary, J. P., & Murtugudde, R. (2005). Impact of Indian Ocean sea surface temperature on developing El Niño. *Journal of Climate*, *18*(2), 302–319. https://doi.org/10.1175/jcli-3268.1

Balmaseda, M. A., Mogensen, K., & Weaver, A. T. (2015). Evaluation of the ECMWF ocean reanalysis system ORAS4. *Quarterly Journal of the Royal Meteorological Society*, *139*, 1132–1161. https://doi.org/10.1002/qj.2063

Baquero-Bernal, A., Latif, M., & Legutke, S. (2002). On dipolelike variability of sea surface temperature in the tropical Indian Ocean. *Journal of Climate*, *15*(11), 1358–1368. https://doi.org/10.1175/1520-0442(2002)015<1358:ODVOSS>2.0.CO;2

Barnston, A. G., Tippett, M. K., van den Dool, H. M., & Unger, D. A. (2015). Toward an improved multimodel ENSO prediction. *Journal of Climate*, *54*, 1579–1595. https://doi.org/10.1175/jamc-d-14-0188.1

Battisti, D. S., Vimont, D. J., & Kirtman, B. (2018). 100 years of progress in understanding the dynamics of coupled atmosphere–ocean variability. *Meteorological Monographs*, *59*(1), 8.1–8.57. https://doi.org/10.1175/AMSMONOGRAPHS-D-18-0025.1

Cai, W., Wu, L., Lengaigne, M., Li, T., McGregor, S., Kug, J.-S., et al. (2019). Pantropical climate interactions. *Science*, *363*(6430), eaav4236. https://doi.org/10.1126/science.aav4236

Chambers, D. P., Tapley, B. D., & Stewart, R. H. (1999). Anomalous warming in the Indian Ocean coincident with El Niño. *Journal of Geophysical Research*, *104*(C2), 3035–3047. https://doi.org/10.1029/1998JC900085

Chang, P., Saravanan, R., & Ji, L. (2003). Tropical Atlantic seasonal predictability: The roles of El Niño remote influence and thermodynamic air-sea feedback. *Geophysical Research Letters*, *30*(10), 1501. https://doi.org/10.1029/2002GL01611910

Chen, C., Cane, M. A., Henderson, N., Lee, D. E., Chapman, D., Kondrashov, D., & Chekroun, M. D. (2016). Diversity, nonlinearity, seasonality, and memory effect in ENSO simulation and prediction using empirical model reduction. *Journal of Climate*, *29*(5), 1809–1830. https://doi.org/10.1175/jcli-d-15-0372.1

Chiang, J. C. H., & Sobel, A. H. (2002). Tropical tropospheric temperature variations caused by ENSO and their influence on the remote tropical climate. *Journal of Climate*, *15*(18), 2616–2631. https://doi.org/10.1175/1520-0442(2002)015<2616:TTTVCB>2.0.CO;2

Curtis, S., & Hastenrath, S. (1995). Forcing of anomalous sea surface temperature evolution in the tropical Atlantic during Pacific warm events. *Journal of Geophysical Research*, *100*(C8), 15835–15847. https://doi.org/10.1029/95JC01502

Ding, H., Keenlyside, N., & Latif, M. (2011). Impact of the equatorial Atlantic on the El Niño Southern Oscillation. *Climate Dynamics*, *38*(9–10), 1–8. https://doi.org/10.1007/s00382-011-1097-y

Ding, H., Newman, M., Alexander, M. A., & Wittenberg, A. T. (2019). Diagnosing secular variations in retrospective ENSO seasonal forecast skill using CMIP5 model-analogs. *Geophysical Research Letters*, *46*, 1721–1730. https://doi.org/10.1029/2018gl080598

Dommenget, D., & Yu, Y. (2017). The effects of remote SST forcings on ENSO dynamics, variability and diversity. *Climate Dynamics*, *49*(7), 2605–2624. https://doi.org/10.1007/s00382-016-3472-1

Dong, L., Zhou, T., & Wu, B. (2014). Indian Ocean warming during 1958–2004 simulated by a climate system model and its mechanism. *Climate Dynamics*, *42*, 203–217. https://doi.org/10.1007/s00382-013-1722-z

Du, Y., & Xie, S. P. (2008). Role of atmospheric adjustments in the tropical Indian Ocean warming during the 20th century in climate models. *Geophysical Research Letters*, *35*, L08712. https://doi.org/10.1029/2008GL033631

Efron, B., & Tibshirani, R. J. (1993). *An introduction to the bootstrap*. Chapman & Hall. https://doi.org/10.1007/978-1-4899-4541-9

Enfield, D. B., & Mayer, D. A. (1997). Tropical Atlantic sea surface temperature variability and its relation to El Niño–Southern Oscillation. *Journal of Geophysical Research*, *102*(C1), 929–945. https://doi.org/10.1029/96JC03296

Frankignoul, C., Gastineau, G., & Kwon, Y. (2017). Estimation of the SST response to anthropogenic and external forcing and its impact on the Atlantic multidecadal oscillation and the Pacific decadal oscillation. *Journal of Climate*, *30*(24), 9871–9895. https://doi.org/10.1175/jcli-d-17-0009.1

Frauen, C., & Dommenget, D. (2012). Influences of the tropical Indian and Atlantic oceans on the predictability of ENSO. *Geophysical Research Letters*, *39*(2). https://doi.org/10.1029/2011GL050520

Ham, Y.-G., Kug, J.-S., & Park, J.-Y. (2013). Two distinct roles of Atlantic SSTs in ENSO variability: North tropical Atlantic SST and Atlantic Niño. *Geophysical Research Letters*, *40*(15), 4012–4017. https://doi.org/10.1002/grl.50729

Izumo, T., Lengaigne, M., Vialard, J., Luo, J. J., Yamagata, T., & Madec, G. (2010). Influence of Indian Ocean dipole and Pacific recharge on following year's El Niño: Interdecadal robustness. *Climate Dynamics*, *42*(1–2), 291–310. https://doi.org/10.1007/s00382-012-1628-1

Jansen, M. F., Dommenget, D., & Keenlyside, N. (2009). Tropical atmosphere-ocean interactions in a conceptual framework. *Journal of Climate*, *22*(3), 550–567. https://doi.org/10.1175/2008jcli2243.1

Kajtar, J. B., Santoso, A., England, M. H., & Cai, W. (2017). Tropical climate variability: Interactions across the Pacific, Indian, and Atlantic oceans. *Climate Dynamics*, *48*, 2173–2190. https://doi.org/10.1007/s00382-016-3199-z

Keenlyside, N., Ding, H., & Latif, M. (2013). Potential of equatorial Atlantic variability to enhance El Niño prediction. *Geophysical Research Letters*, *40*(10), 2278–2283. https://doi.org/10.1002/grl.50362

Keenlyside, N., Kosaka, Y., Vigaud, N., Robertson, A., Wang, Y., Dommenget, D., et al. (2020). basin interactions and predictability. In C. R. Mechoso (Ed.), *Interacting climates of ocean basins: Observations, mechanisms, predictability, and impacts* (pp. 258–292). Cambridge University Press. https://doi.org/10.1017/9781108610995.009

Klein, S. A., Soden, B. J., & Lau, N.-C. (1999). Remote sea surface variations during ENSO: Evidence for a tropical atmospheric bridge. *Journal of Climate*, *12*(4), 917–932. https://doi.org/10.1175/1520-0442(1999)012<0917:RSSTVD>2.0.CO;2

Levine, A. F. Z., & McPhaden, M. J. (2015). The annual cycle in ENSO growth rate as a cause of the spring predictability barrier. *Geophysical Research Letters*, *42*(12), 5034–5041. https://doi.org/10.1002/2015GL064309

Liu, Z., Jin, Y., & Rong, X. (2019). A theory for the seasonal predictability barrier: Threshold, timing, and intensity. *Journal of Climate*, *32*(2), 423–443. https://doi.org/10.1175/JCLI-D-18-0383.1

Luo, J. J., Zhang, R. C., Behera, S. K., Masumoto, Y., Jin, F.-F., Lukas, R., & Yamagata, T. (2010). Interaction between El Niño and extreme Indian Ocean dipole. *Journal of Climate*, *23*(3), 726–742. https://doi.org/10.1175/2009jcli3104.1

Martinez-Villalobos, C., Newman, M., Vimont, D. J., Penland, C., & Neelin, J. D. (2019). Observed El Niño-La Niña asymmetry in a linear model. *Geophysical Research Letters*, *46*, 9909–9919. https://doi.org/10.1029/2019GL082922

Neelin, J. D., Battisti, D. S., Hirst, A. C., Jin, F.-F., Wakata, Y., Yamagata, T., & Zebiak, S. E. (1998). ENSO theory. *Journal of Geophysical Research*, *103*(C7), 14261–14290. https://doi.org/10.1029/97JC03424

Newman, M. (2007). Interannual to decadal predictability of tropical and North Pacific sea surface temperatures. *Journal of Climate*, *20*(11), 2333–2356. https://doi.org/10.1175/JCLI4165.1

Newman, M., & Sardeshmukh, P. D. (2017). Are we near the predictability limit of tropical Indo-Pacific sea surface temperatures? *Geophysical Research Letters*, *44*(16), 8520–8529. https://doi.org/10.1002/2017GL074088

Penland, C., & Matrosova, L. (1998). Prediction of tropical Atlantic sea surface temperatures using linear inverse modeling. *Journal of Climate*, *11*(3), 483–496.

Penland, C., & Sardeshmukh, P. D. (1995). The optimal growth of tropical sea surface temperature anomalies. *Journal of Climate*, *8*(8), 1999–2024. https://doi.org/10.1175/1520-0442(1995)008<1999:TOGOTS>2.0.CO;2

Rayner, N. A., Parker, D. E., Horton, E. B., Folland, C. K., Alexander, L. V., Rowell, D. P., et al. (2003). Global analyses of sea surface temperature, sea ice, and night marine air temperature since the late nineteenth century. *Journal of Geophysical Research*, *108*(D14), 4407. https://doi.org/10.1029/2002JD002670

Rodriguez-Fonseca, B., Polo, I., Garcia-Serrano, J., Losada, T., Mohino, E., Mechoso, C. R., & Kucharski, F. (2009). Are Atlantic Niños enhancing Pacific ENSO events in recent decades? *Geophysical Research Letters*, *36*(20), L20705. https://doi.org/10.1029/2009GL040048

Ruprich-Robert, Y., Msadek, R., Castruccio, F., Yeager, S., Delworth, T., & Danabasoglu, G. (2017). Assessing the climate impacts of the observed Atlantic multidecadal variability using the GFDL CM2.1 and NCAR CESM1 global coupled models. *Journal of Climate*, *30*(8), 2785–2810. https://doi.org/10.1175/JCLI-D-16-0127.1

Shinoda, T., Alexander, M. A., & Hendon, H. H. (2004). Remote response of the Indian Ocean to interannual SST variations in the tropical Pacific. *Journal of Climate*, *17*(2), 362–372. https://doi.org/10.1175/1520-0442(2004)017<0362:RROTIO>2.0.CO;2

Shinoda, T., Hendon, H. H., & Alexander, M. A. (2004). Surface and subsurface dipole variability in the Indian Ocean and its relation with ENSO. *Deep Sea Research Part I Oceanographic Research Papers*, *51*(5), 619–635. https://doi.org/10.1016/j.dsr.2004.01.005

Shin, S.-I., Sardeshmukh, P. D., Newman, M., Penland, C., & Alexander, M. A. (2021). Impact of the annual cycle on ENSO variability and predictability. *Journal of Climate*, *34*(1), 171–193. https://doi.org/10.1175/JCLI-D-20-0291.1

Torrence, C., & Webster, P. J. (1998). The annual cycle of persistence in the El Niño/Southern Oscillation. *Quarterly Journal of the Royal Meteorological Society*, *124*(550), 1985–2004. https://doi.org/10.1002/qj.49712455010

Wang, C. (2019). Three-Ocean interactions and climate variability: A review and perspective. *Climate Dynamics*, *53*, 5119–5136. https://doi.org/10.1007/s00382-019-04930-x

Wang, C., Deser, C., Yu, J. Y., DiNezio, P., & Clement, A. (2017). El Niño and Southern Oscillation (ENSO): A review. In P. Glynn, D. Manzello, & I. Enochs (Eds.), *Coral reefs of the eastern tropical Pacific. Coral Reefs of the World* (Vol. 8, pp. 85–106). Springer. https://doi.org/10.1007/978-94-017-7499-4_4

Wright, P. B. (1979). Persistence of rainfall anomalies in the central Pacific. *Nature*, *277*, 371–374. https://doi.org/10.1038/277371a0

Wu, R., & Kirtman, B. P. (2004). Understanding the impacts of the Indian Ocean on ENSO variability in a coupled GCM. *Journal of Climate*, *17*(20), 4019–4031. https://doi.org/10.1175/1520-0442(2004)017<4019:UTIOTI>2.0.CO;2

Xie, S., Annamalai, H., Schott, F. A., & McCreary, J. P., Jr. (2002). Structure and Mechanisms of South Indian Ocean climate variability. *Journal of Climate*, *15*(8), 864–878. https://doi.org/10.1175/1520-0442(2002)015<0864:SAMOSI>2.0.CO;2

Yuan, D., Wang, J., Xu, T., Xu, P., Hui, Z., Zhao, X., et al. (2011). Forcing of the Indian Ocean dipole on the interannual variations of the tropical Pacific Ocean: Roles of the Indonesian throughflow. *Journal of Climate*, *24*(14), 3593–3608. https://doi.org/10.1175/2011JCLI3649.1

Yuan, D., Zhou, H., & Zhao, X. (2013). Interannual climate variability over the tropical Pacific Ocean induced by the Indian Ocean dipole through the Indonesian throughflow. *Journal of Climate*, *26*(9), 2845–2861. https://doi.org/10.1175/JCLI-D-12-00117.1

Zhang, L., Wang, G., Newman, M., & Han, W. (2021). Interannual to decadal variability of tropical Indian Ocean sea surface temperature: Pacific influence versus local internal variability. *Journal of Climate*, *34*(7), 2669–2684. https://doi.org/10.1175/JCLI-D-20-0807.1

Zhao, Y., Newman, M., Capotondi, A., Di Lorenzo, E., & Sun, D. (2021). Removing the effects of tropical dynamics from North Pacific climate variability. *Journal of Climate*, *34*(23), 9249–9265. https://doi.org/10.1175/JCLI-D-21-0344.1

Zhou, Q., Mu, M., & Duan, W. (2019). The initial condition errors occurring in the Indian Ocean temperature that cause "spring predictability barrier" for El Niño in the Pacific Ocean. *Journal of Geophysical Research: Oceans*, *124*(2), 1244–1261. https://doi.org/10.1029/2018JC014403

References From the Supporting Information

Battisti, D. S., & Hirst, A. C. (1989). Interannual variability in a tropical atmosphere–ocean model: Influence of the basic state, ocean geometry and nonlinearity. *Journal of the Atmospheric Sciences*, *46*(12), 1687–1712. https://doi.org/10.1175/1520-0469(1989)046<1687:IVIATA>2.0.CO;2

Compo, G. P., & Sardeshmukh, P. D. (2010). Removing ENSO-related variations from the climate record. *Journal of Climate*, *23*(8), 1957–1978. https://doi.org/10.1175/2009JCLI2735.1

Farrell, B. (1988). Optimal excitation of neutral Rossby waves. *Journal of the Atmospheric Sciences*, *45*(2), 163–172. https://doi.org/10.1175/1520-0469(1988)045<0163:OEONRW>2.0.CO;2

Jin, F.-F. (1997). An equatorial ocean recharge paradigm for ENSO. Part I: Conceptual model. *Journal of the Atmospheric Sciences*, *54*(7), 811–829. https://doi.org/10.1175/1520-0469(1997)054<0811:AEORPF>2.0.CO;2

Lacarra, J.-F., & Talagrand, O. (1988). Short-range evolution of small perturbation in a barotropic model. *Tellus A: Dynamic Meteorology and Oceanography*, *40*(2), 81–95. https://doi.org/10.3402/tellusa.v40i2.11784

Meinen, C. S., & McPhaden, M. J. (2000). Observations of warm water volume changes in the equatorial Pacific and their relationship to El Niño and La Niña. *Journal of Climate*, *13*(20), 3551–3559. https://doi.org/10.1175/1520-0442(2000)013<3551:OOWWVC>2.0.CO;2

Penland, C., & Matrosova, L. (2006). Studies of El Niño and interdecadal variability in tropical sea surface temperatures using a nonnormal filter. *Journal of Climate*, *19*(22), 5796–5815. https://doi.org/10.1175/JCLI3951.1